Organic Process Research & Development

Article

pubs.acs.org/OPRD

Optimization of the Preparation of (*R*)-3,5-Bis(trifluoromethyl)-α-methyl-*N*-methylbenzylamine L-(−)-Malic Acid Salt through Classical Resolution

Clément M. Brandel, Jason W. B. Cooke, Richard A. J. Horan, Franck P. Mallet, and David R. Stevens*

Global API Chemistry, GlaxoSmithKline Research and Development, Medicines Research Centre, Gunnels Wood Road, Stevenage, Hertfordshire, SG1 2NY, United Kingdom

ABSTRACT: An improved process for the manufacture of (*R*)-3,5-bis(trifluoromethyl)-α-methyl-*N*-methylbenzylamine L-(−)-malic acid salt (**1**), a key starting material for many pharmaceutical targets, is described. Rapid process understanding for the synthesis of the racemic benzylamine was achieved by the use of time coursing studies and design of experiments (DoE). Preferred conditions for resolution of the pure diastereomer with L-(−)-malic acid were readily determined through the consideration of ternary phase diagrams. These were simply constructed from a series of single solubility experiments that allowed the rapid screening and evaluation of the resolution conditions. Optimized conditions, practical operating ranges, and their robustness for use in manufacturing were confirmed by the use of DoE resulting in product with diastereomeric purity of >99%. For this resolution, it was shown that a further recrystallization was necessary to achieve a chiral purity of >99.9%. The new process offers significant advantages in terms of operational simplicity, robustness, and freedom to operate and has been successfully carried out at the intended commercial scale.

INTRODUCTION

The L-(−)-malic acid salt of (*R*)-3,5-bis(trifluoromethyl)-α-methyl-*N*-methylbenzylamine **1** or the free base **3** (Figure 1) are important chiral building blocks used in the synthesis of a number of NK-1 receptor antagonists. These active pharmaceutical ingredients (APIs) have been in development for the treatment of a range of conditions including postoperative nausea and vomiting (PONV), chemotherapy induced nausea and vomiting (CINV), anxiety, and depression. Salt **1** is a proposed registered starting material (RSM) for vestipitant[1] **4**, and the free base **3** was previously proposed as a RSM for the related NK-1 antagonists casopitant[2] **5** and orvepitant[3] **6** (Figure 1).

Although **1** fulfils virtually all of the criteria for RSMs as set out in ICH Q11,[4] its use in the final stage of vestipitant **4** synthesis (Scheme 1) is a major project risk. This stage isolates clinical-grade API directly but offers poor control of the impurity that may be formed due to the presence of diastereomer **2**, which results in stringent specification requirements for this impurity (i.e., < 0.15%). Consequently, a robust stereoselective route for the production of **1** is required.

Enantiomerically enriched free base **3** can be prepared as an oil by asymmetric synthesis via a number of commercial and literature reported routes (Scheme 2). Hodges et al.[5] reported the asymmetric reduction of commercially available 3′,5′-bis(trifluoromethyl)acetophenone **11** to the chiral alcohol **12** under hydrogenation or enzymatic conditions followed by displacement of the corresponding mesylate **13** with methylamine. In recent years, many other new highly stereoselective reductions of ketones have been reported as exemplified by the asymmetric hydrogenation reported by Xie et al.[6] using an iridium catalyst with a SpiroPAP ligand **21** delivering **12** with ee of 99.9%. Tanaka et al.[7] reported that the chiral alcohol can be displaced under Mitsunobu conditions with sulfonamide **22** to give **14**, and the chiral amine can be liberated under basic conditions in the presence of a thiol. Ishii et al.[8] prepared the imine **15** with the chiral auxiliary (*R*)-(+)-α-methylbenzylamine **23**, which was then selectively reduced to **16** (a number of conditions have been reported, one of which is shown in Scheme 2) followed by methylation and debenzylation to give **3**. Achiral imine **17** was selectively reduced by Jones and Li[9] using trichlorosilane in the presence of organocatalyst **24**. This imine was also reduced at DSM using an iridium catalyst containing the chiral ferrocene ligand **25** under hydrogenation conditions.[10] The stereoselective hydrogenation of enamide **19** to **20** in exceptional enantiomeric excess using rhodium complexes of chiral phosphines (as exemplified by (R,R)-QuinoxP* **26**) has also been recently demonstrated by Imamoto and Gridnev.[11]

These routes suffer from three main issues:

- The use of proprietary technologies for the reduction step which could complicate registration with the regulatory authorities and present risks with freedom to operate.
- The potential for a higher level of operational complexity, which might impact robustness, carbon footprint, and cost of materials and reagents.
- They generally give material of enantiomeric purity which is below the desired specification (i.e., ≥99.7% ee), requiring an additional enantiopurification procedure.

During the initial development work on **4** at GSK, diastereomeric salt **1** had been prepared using a non-

Received: February 18, 2015

DOI: 10.1021/acs.oprd.5b00283
Org. Process Res. Dev. XXXX, XXX, XXX−XXX

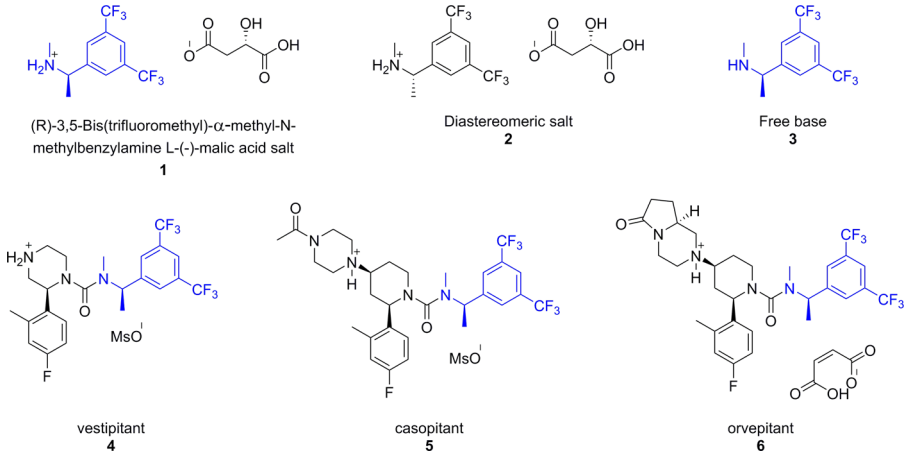

Figure 1. (*R*)-3,5-Bis(trifluoromethyl)-*α*-methyl-*N*-methylbenzylamine versions and APIs containing this structural element.

Scheme 1. Synthesis of Vestipitant (4)[a]

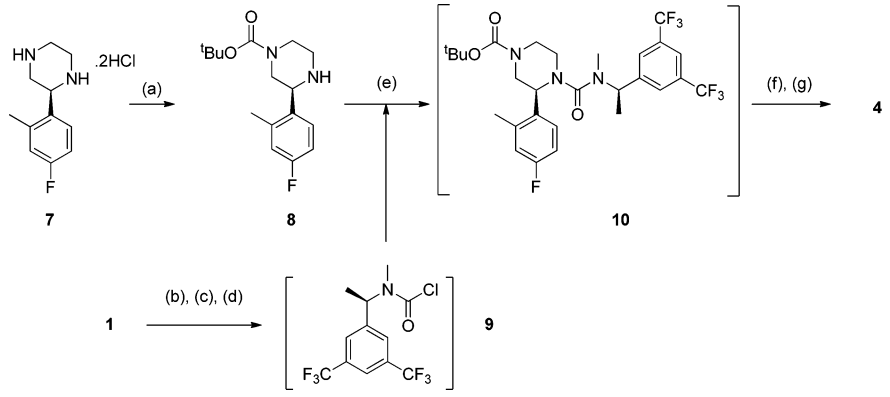

[a](a) Boc_2O, Et_3N, EtOAc; (b) Na_2CO_3, EtOAc; (c) CO_2, Et_3N, TMSCl; (d) $SOCl_2$, pyridine; (e) Et_3N, EtOAc; (f) CH_3SO_3H, EtOAc; (g) CH_3SO_3H, EtOAc, iso-octane.

stereoselective reductive amination followed by resolution of the racemic mixture **27** (Scheme 3).

This route is not subject to any IP restrictions, so its use would simplify inclusion in a regulatory file if required. Despite the inherent yield limit imposed by the resolution approach, its brevity and operational simplicity would also potentially offer a significant saving in cost and cycle time if a robust and efficient resolution process could be developed.

Chiral Resolutions. Among resolution techniques such as chiral chromatography, preferential crystallization,[12] Viedma ripening,[13] or preferential enrichment,[14] the Pasteurian resolution technique[15] was identified as the most suitable method for the resolution of **3** and the preparation of **1**.[16] This crystallization technique, based on the symmetry breaking of enantiomers of **3** by the formation of the diastereomeric salts **1** and **2**, can be easily implemented but requires a preliminary knowledge of the types of heterogeneous equilibria existing in the ternary system between **1**, **2** and the selected solvent, which are best understood with the use of phase diagrams. Phase diagrams are graphical representations of the phase behavior of the constituents of the system as a function of chemical composition and intensive variables (e.g., temperature or pressure).[17] They are useful tools for the design of crystallization protocols and are widely used in the field of chiral resolution by crystallization.[18]

Considering a ternary system consisting of two diastereomeric salts A and B and a solvent, it is possible to represent the different heterogeneous equilibria occurring in the system at fixed temperature and pressure in an equilateral triangle. Several situations can be envisaged and those most usually encountered are illustrated in Figure 2. Figure 2a shows the ideal targeted situation for a Pasteurian resolution process in which opposite diastereomeric salts A and B crystallize separately: they self-resolve via crystallization. The principle of the Pasteurian resolution of salt B consists of conducting a crystallization starting with an equimolar mixture of both diastereomeric salts and adjusting the composition of the system to reach the blue domain (Figure 3), in which a slurry of pure salt B is in equilibrium with a saturated solution enriched in salt A, while evolving on the so-called isoplethal section (bold line in Figure 3). From Figure 2b, one can see that this resolution cannot occur in the case that a double salt AB (i.e., a defined compound) presenting a congruent solubility[19] is formed since it is not possible to bring the system to the blue domain while evolving on the isoplethal section. In contrast, if the double salt AB has a noncongruent solubility (Figure 2c), Pasteurian resolution remains possible. Figure 2d depicts the existence of a complete solid solution between salts A and B, i.e., a crystal structure that does not discriminate A or B, for which Pasteurian resolution is impossible. The complexity of these phase diagrams can increase if one of the system components

DOI: 10.1021/acs.oprd.5b00283
Org. Process Res. Dev. XXXX, XXX, XXX−XXX

Scheme 2. Literature Synthetic Strategies of Bis(trifluoromethyl)-α-methyl-*N*-methylbenzylamines[a]

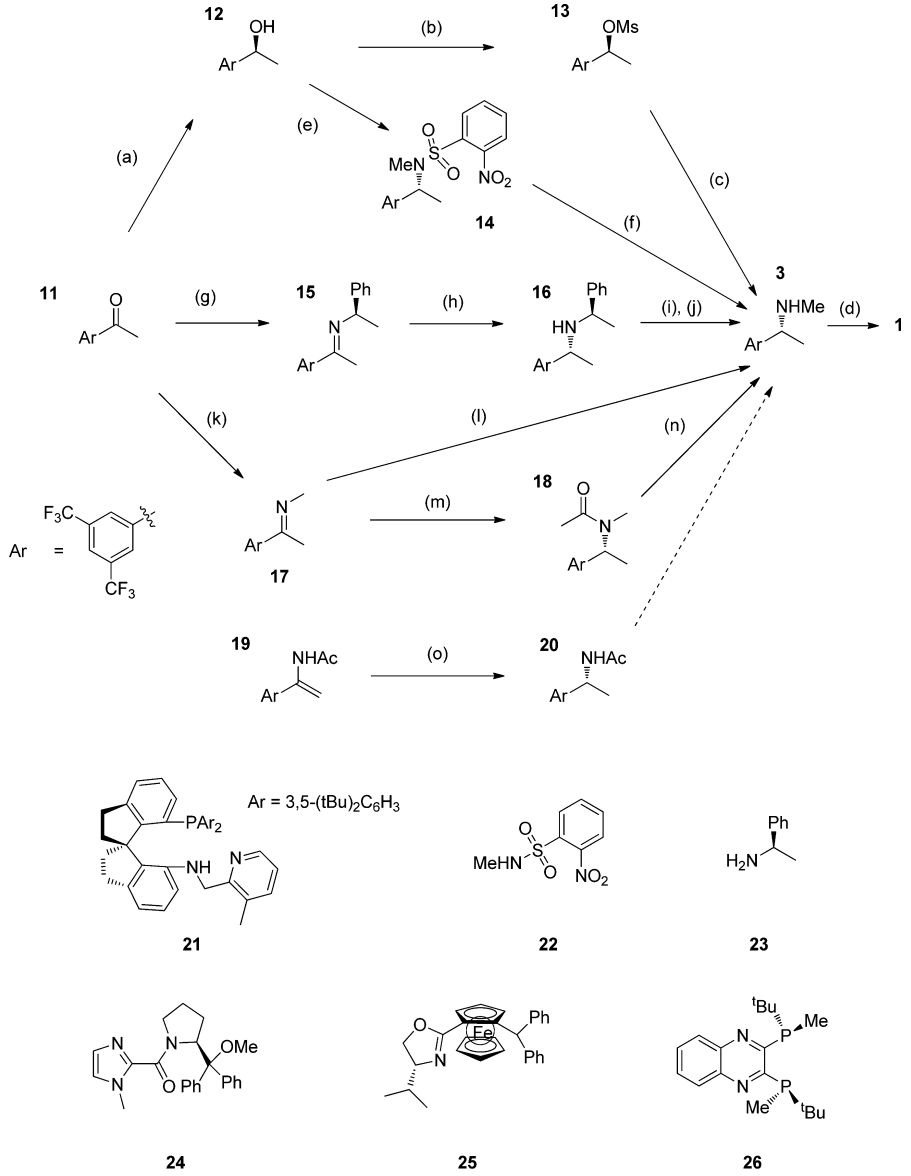

[a](a) Rh, Ru, or Ir chiral catalyst, Et_3N, HCOOH, THF, or *Geotrichum candidum* BPCC 1118 or H_2, [{Ir(COD)Cl}$_2$]/**21**, S/C 5000, EtOH, KO^{t}Bu, 10 atm, rt ; (b) MsCl, Et_3N; (c) $MeNH_2$; (d) L-(−)-malic acid; (e) DIAD, PPh_3, **22**; (f) 3 M NaOH (3 eq), *n*-dodecanethiol (1.1 eq), TBAB (0.1 eq), 20−25 °C; (g) $ZnCl_2$, **23**; (h) H_2, 5% Pt/alumina, MeOH, 25 °C, 10 bar; (i) paraformaldehyde, H_2, 100 °C, 20 bar; (j) H_2, AcOH, 5% Pd/C, 60 °C, 0.5 MPa; (k) CH_3NH_2, Ti(OiPr)$_4$, or 40% CH_3NH_2 in MeOH, pTSA, Na_2SO_4; (l) EtOAc, **24**, 0 °C, $HSiCl_3$ (2 eq), (m) Ac_2O (1.1 eq), [Ir(COD)Cl]$_2$, **25**, I_2, H_2, 25 bar, (n) HCl (6 N), PrOH, (o) H_2, [Rh((R,R)-QuinoxP*) (cod)]SbF_6, S/C 10000, MeOH, 5 atm, rt, 20 h, 99.9% ee.

Scheme 3. Resolution Route to 1

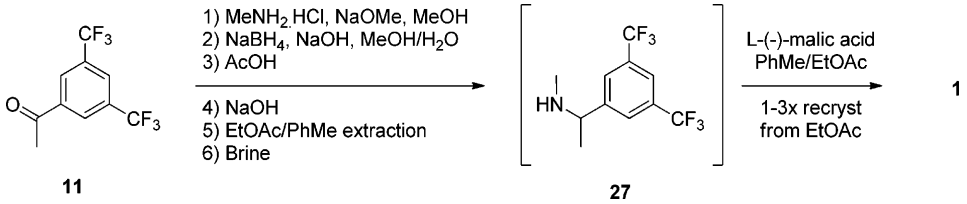

presents polymorphism, exists as a solvate, if the system presents terminal solid solutions, or if metastable (or stable) states, in which the system behaves differently with regard to chiral discrimination, can be reached. These situations have been comprehensively described by Marchand et al.[20] and will not be considered in this paper.

Provided a system such as depicted in Figure 2a is found, Figure 3 underlines the central importance of determining the composition of the eutectic point E (composition of a doubly saturated solution) and frontier point F (composition where the system consists of a slurry exhibiting maximal amount of pure salt B crystals in suspension and maximal amount of

DOI: 10.1021/acs.oprd.5b00283
Org. Process Res. Dev. XXXX, XXX, XXX−XXX

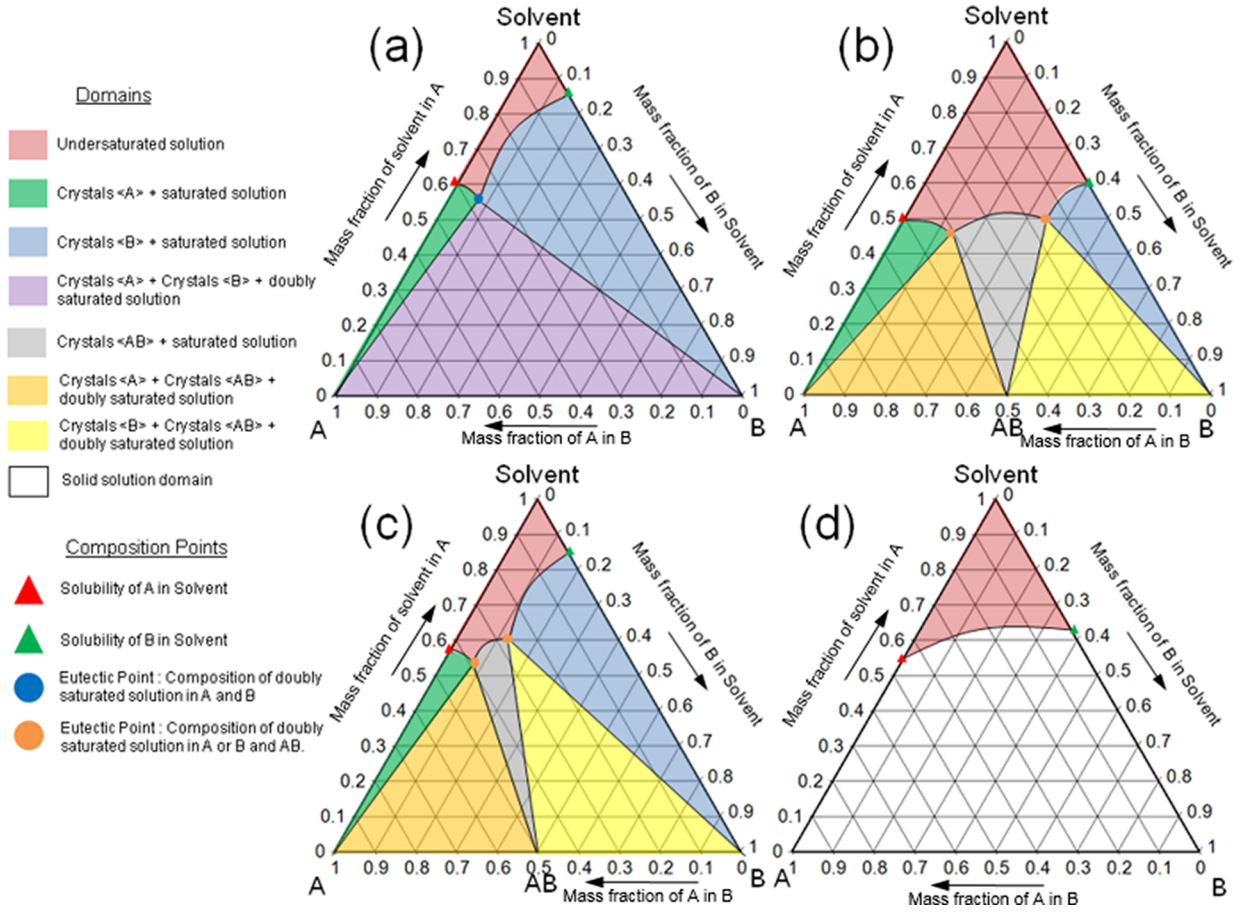

Figure 2. Schematic representations of ternary phase diagram between two diastereomeric salts A and B and a solvent illustrating the occurrence of: (a) complete discrimination at the solid state, (b) existence of a double salt with congruent solubility, (c) with noncongruent solubility, and (d) a complete solid solution.

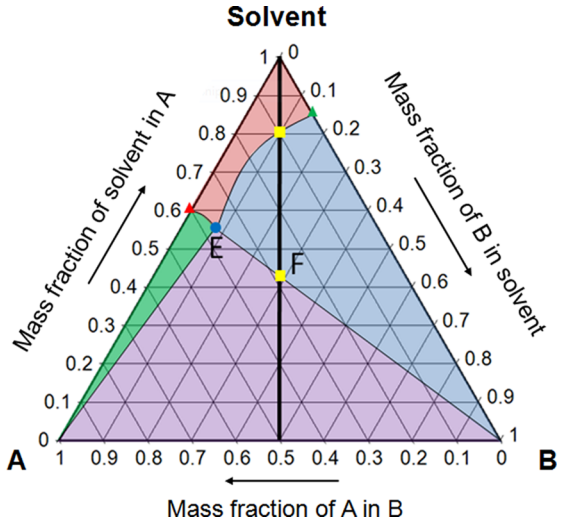

Figure 3. Principle of the Pasteurian resolution of an equimolar mixture of diastereomers. Refer to Figure 2 for color code.

dissolved salt A, i.e., where resolution is optimal) to design the resolution process.

Eutectic point E, with chemical composition

$(W_A^E, W_B^E, W_{solvent}^E)$ in %wt

can be determined by analyzing the composition of the mother liquor of a slurry whose composition lies in the purple domain of Figure 3 (i.e., a slurry of both salt A and B) and then used to determine the phase boundary BE. Reporting W_A and W_B in an orthonormal base (0, x, y) such as in Figure 4, the equation of BE (purple line in Figure 4) is:

$$W_A = \frac{-W_A^E}{100 - W_B^E} W_B + \frac{100 W_A^E}{100 - W_B^E} \quad (1)$$

Point F, with chemical composition

$(W_A^F, W_B^F, W_{solvent}^F)$ in %wt

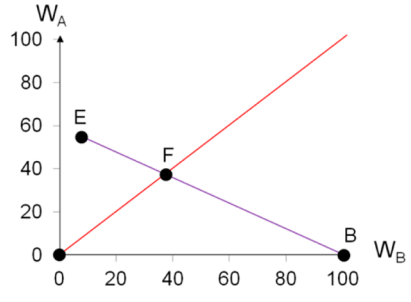

Figure 4. Phase boundary BE (purple) and the isoplethal section AB–S (red) expressed in an orthonormal basis.

DOI: 10.1021/acs.oprd.5b00283
Org. Process Res. Dev. XXXX, XXX, XXX−XXX

is the intersection between boundary BE and the perpendicular bisection line of the ternary phase diagram (AB−S isoplethal section, bold line in Figure 3, red line in Figure 4) whose equation in the orthonormal base is:

$$W_B = W_A \quad (2)$$

Therefore, W_A^F and W_B^F can be determined by solving simulateneously eqs 1 and 2, giving:

$$W_A^F = W_B^F = \frac{100W_A^E}{100 - W_B^E + W_A^E} \quad (3)$$

and $W_{solvent}^F$ is given by

$$100 - \left(2\frac{100W_A^E}{100 - W_B^E + W_A^E}\right) \quad (4)$$

The minimal amount of solvent required to fully dissolve salt A from an equimolar mixture of both diastereomeric salts can easily be calculated:

$$\frac{100 - W_B^E - W_A^E}{2W_A^E d_{solvent}} \quad (\text{in mL/g}) \quad (5)$$

with $d_{solvent}$ the density of the chosen solvent.

The theoretical mass of salt B collected after the resolution process of m gram of the equimolar mixture of diastereomeric salts, i.e., the expected recovery, is given by:

$$\frac{m(W_A^E - W_B^E)}{2W_A^E} \quad (6)$$

As a rule of thumb, resolving agent and solvent selection should be driven by the search for a large solubility difference between the diastereomers A and B, in order to afford an easier process and a higher yield. It is also worth checking for the existence of terminal solid solutions as these might result in poor enantiomeric purity of the final material.

The aim of this paper is to describe how an operationally simple process for the production of **1**, providing substantial savings to the cost of goods and carbon footprint and relying on a robust and efficient Pasteurian resolution procedure, was developed in a pharmaceutical environment.

RESULTS AND DISCUSSION

Preparation of the Racemic Mixture 27. An initial survey indicated that, in addition to the hydrochloride salt, methylamine (starting material for this synthesis) was commercially available as a pure material (gas, bp −6 °C) or as a solution in methanol, ethanol, THF, or water. The solutions were much preferred over the pure material for handling reasons, and the imine formation was found to proceed efficiently in methanol or ethanol but gave poor results in THF. Further investigation established that purchasing solutions of methylamine in alcohols would require custom preparation with the associated additional cost; however, the aqueous solution (40% w/w) is a commodity material, readily available in bulk at low cost. Although the presence of water might be expected to adversely impact the position of the equilibrium during imine formation, a test reaction using this aqueous methylamine in methanol as reaction solvent gave a comparable profile to using a solution in ethanol. We therefore selected the aqueous solution for further development with the proposed reaction sequence outlined in Scheme 4.

Scheme 4. Proposed Imine Formation and Reduction[a]

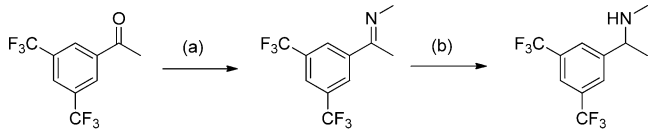

11 17 27

[a](a) $MeNH_2$ (40% aq); (b) $NaBH_4$

The first step was to undertake a solvent screen for imine formation using a PCA[1] solvent model (Table 1) to select a diverse set of solvents that was augmented with additional alcohols based on our previous experience. Acetophenone derivative **11** and aqueous methylamine (40% w/w) (2.5 eq) were stirred in solvent (2 mL/g) at ambient temperature overnight, and then the conversion to the imine was measured by ^{1}H NMR (Table 1).[21]

These results show a very strong solvent dependence for the reaction with alcohols (particularly methanol) giving the best results. Although a small amount of water (from the methylamine solution) is tolerated, it unsurprisingly gave poor results when used as the sole solvent.

We next examined the effect of pH on the imine formation. Lowering the pH of the system (by substituting a portion of the methylamine with the equivalent amount of the HCl salt) accelerated the imine formation as expected but also shifted the equilibrium point toward the starting materials. In addition, lower pH led to problems with foaming during the reduction step, and so this option was not pursued further.

With reagents and solvents selected we next sought to optimize reaction variables through the use of design of experiments (DoE). Variables selected were the amount of 40% $MeNH_2$ (2−3 equiv relative to **11** (1.0 equiv)), concentration (2−6 mL/g in methanol), and temperature (15−25 °C). Responses were the conversion after 1 h (to give an indication of the kinetics of the reaction) and 24 h (to give an indication of the equilibrium position) as measured by ^{1}H NMR. Results indicated that increasing the temperature resulted in a faster initial reaction as expected but a lower conversion at equilibrium. A larger excess of methylamine favored the conversion at both times, while the amount of methanol solvent had little effect within the range investigated. The results also indicated that there was significant curvature in the responses so a follow-up central composite design (Table 2) allowed us to explore the impact of reagent equivalents and temperature in more detail (Figure 5). In this case the intermediate imine **17** was reduced to the amine **27** by addition of sodium borohydride and was analyzed by HPLC. Results showed good correlation with the conversion to the intermediate imine which was determined by GC.

These results suggested that allowing the imine formation reaction to reach equilibrium at a higher temperature and then cooling it to displace the equilibrium toward the desired product would give the best conversion in the shortest time. In order to determine the amount of time required for each phase of the reaction to reach equilibrium, two time-course experiments were run. The first (Figure 6a) measured the conversion to the imine at 30 °C which showed conversion approaches equilibrium of ∼ 95% after 8 h. The second (Figure 6b) allowed the reaction to come to equilibrium at 40 °C (∼94% conversion) before rapidly cooling to −5 °C ($t_{-5°C}$ = 0)

DOI: 10.1021/acs.oprd.5b00283
Org. Process Res. Dev. XXXX, XXX, XXX−XXX

Table 1. Solvent Screen of Imine Formation (Conversion Measured by ^{1}H NMR)

solvent	MeOH	EtOH	iPrOH	tBuOH	MeCN	EtOAc	THF	DMSO	water	cyclohexane	TBME	toluene
conversion (%)	94	92	78	60	29	18	10	8	6	2	2	1

Table 2. Central Composite Design for Imine Formation and Reduction to Amine

	factors		responses	
entry	40% $MeNH_2$ (equiv)	temperature (°C)	conversion to **17** at 24 h (% a/a by GC)	**27** (% a/a by HPLC)
1	2	0.0	94.6	94.1
2	4	0.0	97.3	96.6
3	2	25.0	92.6	91.3
4	4	25.0	95.8	94.0
5	1.6	12.5	92.0	91.0
6	4.4	12.5	96.9	95.7
7	3	−5.2	96.9	96.1
8	3	30.2	94.3	92.5
9	3	12.5	95.9	95.1
10	3	12.5	95.8	94.6

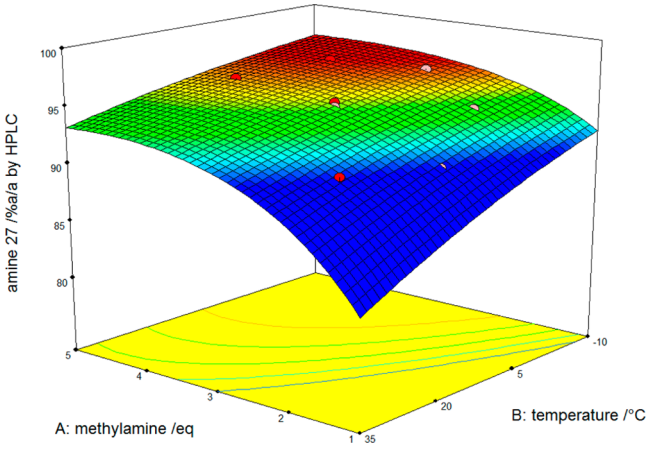

Figure 5. Results from central composite design.

and again monitoring the further conversion to the imine, reaching >98% after 24 h.

The final selected conditions for the imine formation were to dissolve **11** in methanol (6 mL/g) and to react with 40% (w/w) methylamine (3.3 equiv) at 35 ± 5 °C for 6 h. This solution was cooled to 0 ± 5 °C over 2 h and was allowed to reach equilibrium over 10 h.

With the imine formation well understood, we turned our attention to the reduction. Early studies had indicated that adding a freshly prepared solution of sodium borohydride in methanol containing a small amount of sodium hydroxide (as a stabilizer) worked well, but commercial solutions of sodium borohydride in (more concentrated) aqueous sodium hydroxide solution gave poor reaction profiles. Small-scale trials with solid sodium borohydride showed complete reaction when 0.8 equiv was added as a single portion. Portion-wise addition on scale-up (to manage the heat and gas evolution) resulted in incomplete reaction, but this could be overcome by using a larger excess of reagent (1.2 equiv).[22] Subsequent process safety studies provided the heat and gas flow measurements, which allowed calculation of the number and size of the charges required during scale-up in the pilot plant.

Following complete reaction, the remaining hydride species were remarkably stable and did not fully decompose even under reflux, presumably due to the basic pH of the mixture. The addition of acid allowed the hydride species to be decomposed in a controlled manner, and the racemic product could then be obtained after a distillation to remove methanol, neutralization with base and extraction into ethyl acetate. This distillation was important as it allowed the product to be efficiently recovered from the aqueous phase in a single extraction with good phase separation; however, an initial trial using acetic acid (used in the historical process) resulted in a low yield due to losses of product (~25% of the total) to the distillate during MeOH removal. Switching to sulfuric acid resolved this issue, and a change from sodium hydroxide to ammonia in the subsequent neutralization improved the phase separations and minimized the amount of inorganics remaining in the organic phase. A final water wash removed residual traces of inorganics, and this was followed by an azeotropic distillation to remove water (critical for the subsequent crystallization) with only small amounts of the steam volatile **27** (~1% of the total) lost to the distillate.

Due to the simplicity of the new process (Scheme 5) and the level of scientific understanding, no robustness studies were undertaken, and after only 5 runs at 20−100 g scale, the reaction was scaled up to a 20 L reactor (2 batches using 1 kg of **11**) and then to the pilot plant (4 × 50 kg batches, vide infra) without issue.

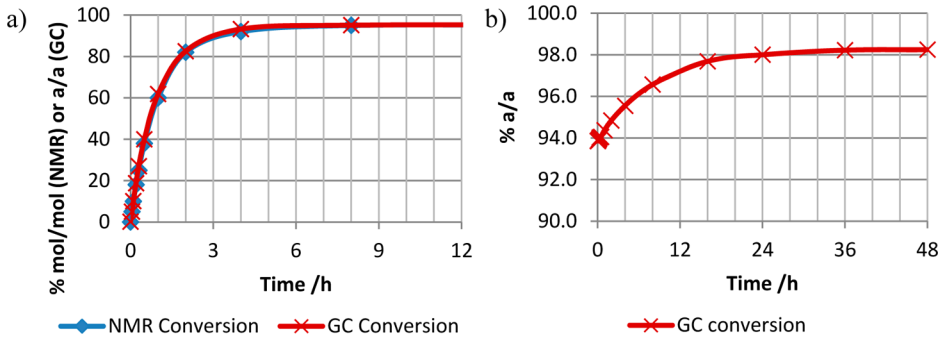

Figure 6. Formation of imine **17**: (a) reaction at 30 °C; (b) imine formation was allowed to come to equilibrium at 40 °C before being cooled to −5 °C ($t_{-5°C}$ = 0).

DOI: 10.1021/acs.oprd.5b00283
Org. Process Res. Dev. XXXX, XXX, XXX−XXX

Scheme 5. Final Process to 27 Solution in Ethyl Acetate

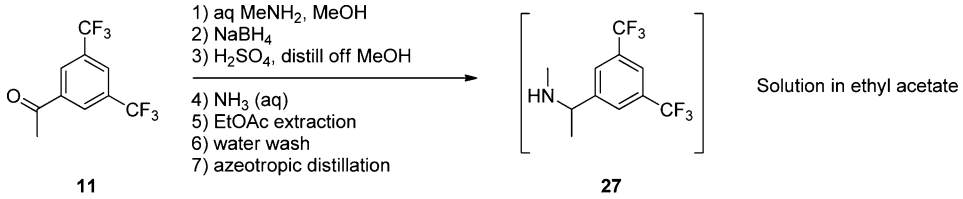

Scheme 6. Resolution of 27.

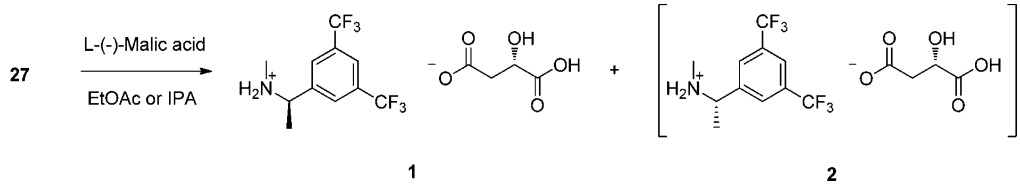

Pastereurian Resolution of 27. *Investigation of the "1−2" Binary System.* The resolution of **27** to **1** is shown in Scheme 6. Before attempted optimization of this resolution, initial studies were performed to confirm the nature of the system. A sample of **2** was prepared by resolution of the racemate **27** with D-(+)-malic acid in ethyl acetate followed by a further recrystallization from ethyl acetate. The free base (*S*)-3,5-bis(trifluoromethyl)-*α*-methyl-*N*-methylbenzylamine was liberated in ethyl acetate solution using aqueous ammonia. The recovered product was dissolved in fresh ethyl acetate and equimolar quantity of L-(−)-malic acid was added. The solution was concentrated; **2** was crystallized by addition of *tert*-butyl methyl ether, and the slurry formed was cooled to −5 °C. After filtration, the solid was washed with tBME and dried. The sample showed <0.05% of diastereomer **1** as determined by chiral GC.

Figure 7 shows the X-ray powder diffractograms (XRPD) of powdered samples of the pure L-(−)-malic acid salts **1** (the targeted salt) and **2**. The differences between the two XRPD patterns confirm that the corresponding crystal structures are different and that the symmetry between enantiomers of **27** is broken. The XRPD signal recorded from a recrystallized equimolar mixture of both salts **1** and **2** (obtained by evaporation to dryness of an ethyl acetate solution) is also shown in Figure 7 and presents peaks characteristic to both **1** and **2** crystals. Therefore, it is confirmed that the system "**1**−**2**" does not present any double salt and that (L)-(-)-malic acid is a resolving agent of **27**.

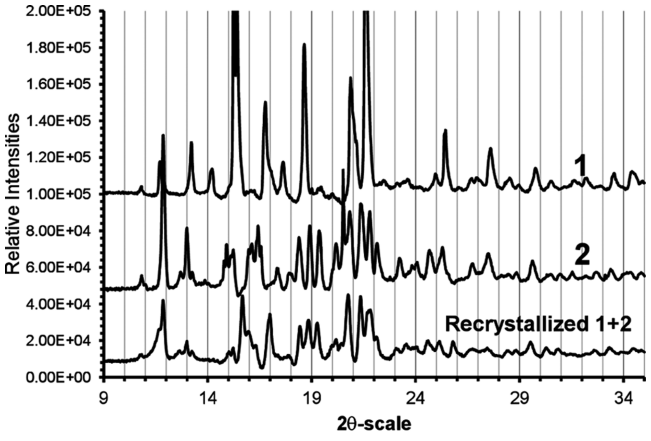

Figure 7. X-ray powder diffractograms of **1**, **2**, and recrystallized equimolar mixture of **1** and **2**. The raw signals were corrected from the background noise due to the sample-holder capton.

To further support our conclusion, each powder was also analyzed by differential scanning calorimetry (DSC). The DSC thermogram of powdered **1** is shown in Figure 8a and presents a single melting peak at T_{onset} = 125.1 °C, and the different melting point obtained for **2** (Figure 8b, T_{onset} = 73.0 °C) is consistent with XRPD analyses. The large difference in melting points of the two salts is consistent with large differences in solubility.[23] Due to its very high stereochemical purity, the asymmetric shape of the melting peak of **2** cannot result from the occurrence of a eutectic melting but can be due to inhomogeneities in the crystalline sample. The thermogram of the recrystallized mixture of **1** and **2** (Figure 8c) presents the typical profile of a succession of eutectic (T_{onset} = 61.3 °C) and liquidus (T_{end} = 110.1 °C) meltings, thus supporting that no double salt is formed (in that case a single melting peak would have been observed) and that **1** and **2** are resolved by L-(−)-malic acid.

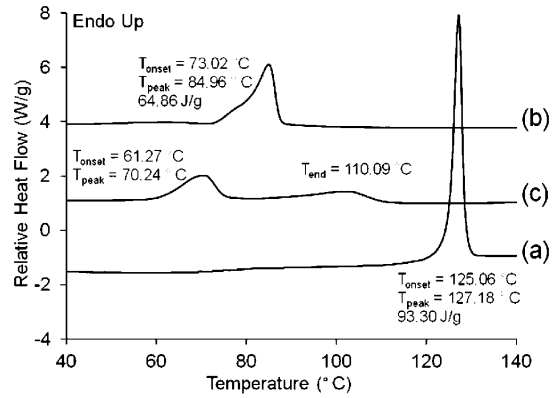

Figure 8. Thermograms of powdered **1** (a), **2** (b), and recrystallized mixture of **1** and **2** (c). The heating rate is 10 °C/min.

*Determination of Points **E** and **F** in the Ternary Systems "**1**−**2**-Ethyl Acetate" and "**1**−**2**-Isopropyl Alcohol".* To determine the eutectic point **E** (Figure 3) at various temperatures, mixtures of the pure diastereomeric salts **1** and **2** (0.5 g of each, chemical purity ∼ 100%) were slurried at different temperatures (Table 3) in 3 mL of either ethyl acetate

DOI: 10.1021/acs.oprd.5b00283
Org. Process Res. Dev. XXXX, XXX, XXX−XXX

Table 3. Compositions of the Equilibrium Doubly Saturated Solutions of 1 and 2, Prepared in Ethyl Acetate or Isopropyl Alcohol at Different Temperatures

		composition (% wt)		
solvent	temperature (°C)	**1**	**2**	solvent
EtOAc	2.5	0.465	1.515	98.02
	10	0.715	2.205	97.08
	20	1.346	4.124	94.53
iPrOH	2.5	7.452	15.908	76.64
	20	6.701	16.169	77.13

or isopropyl alcohol and were stirred over 4 days to ensure that stable equilibria are reached. After sedimentation of the slurry, the mother liquors were collected, syringe filtered, and subsequently analyzed by HPLC to determine the overall concentration of dissolved salts (**1** + **2**) and by chiral GC to determine the stereoisomeric ratio. Table 3 shows the results of our measurements of the compositions of these doubly saturated solutions.

From these single point measurements, the minimal amount of solvent required to fully dissolve **2** was calculated using eq 5 (Table 4).

Table 4. Summary of Calculated Solvent Volumes and Predicted Yields

entry	solvent	temp. (°C)	min. vol.[a] (mL/g)	yield (%)	comment
1	EtOAc	2.5	36.3	34.7	too dilute
2	EtOAc	10	24.7	33.8	too dilute
3	EtOAc	20	12.7	33.7	chosen to develop
4	iPrOH	2.5	3.1	26.6	too soluble
5	iPrOH	20	3.0	29.3	too soluble

[a]Minimum volume of solvent required to dissolve **2** in a 1:1 mixture of diastereomers **1** and **2**.

From these measurements, isopropyl alcohol was dismissed on the basis of the high solubilities of **1** and **2** and the lower expected recovery of **1** in comparison to ethyl acetate, which was therefore selected for the resolution protocol. The temperature of crystallization was fixed at 20 °C, based on the best balance between high recovery and suitable minimal volume of solvent.

Using the knowledge of point **F** in ethyl acetate at 20 °C (12.7 mL/g, Table 4), a resolution trial was performed based on the chosen conditions: L-(−)-malic acid (1 equiv) was added to a solution of the racemic free base **27** (chemical purity ∼98%) in 15 mL/g (vs total weight of **27** plus L-(−)-malic acid) ethyl acetate and dissolved by heating at 60 °C. The solution was rapidly cooled down to 50 °C, seeded with pure **1**, aged for 30 min to establish crystallization, and then cooled down to 20 °C at 0.5 °C/min. The slurry was then seeded with the undesired diastereomer **2** to check that the resolution was under thermodynamic control and that crystallization of the undesired diastereomer would not occur. After further 2.5 h of aging, the slurry was filtered and washed. The yield was 37.8%, and the content of undesired diastereomer **2** was 1.1% a/a as determined by GC.

Unexpectedly, we have observed that similar resolution trials performed using as low as 7.5, 10, and 12.5 mL/g ethyl acetate (i.e., <12.7 mL/g − entries 1, 2, and 3 in Table 5) were also

Table 5. Experimental Results Obtained for the Resolution Experiments Using Different Amounts of Solvent

entry	EtOAc[a] (mL/g)	temperature (°C)	seed at 50 °C	seed at final temp.	yield (%)	diastereomer **2** (% a/a by GC)
1	7.5	20	**1**	**2**	37.9	1.2
2	10	20	**1**	**2**	38.1	1.2
3	12.5	20	**1**	**2**	37.8	1.2
4	15	20	**1**	**2**	37.3	1.1
5	5	−2.5	**1**	none	41.0	1.3
6	10	2.5	**2**	**2**	60.0	30.8

[a]Weight based on 1:1 mixture of diastereomers **1** and **2**.

successful in delivering crystals of **1** with strikingly high stereoisomeric purity and comparable yields. The 4% yield discrepancy between theoretical prediction (Table 4) and experimental results could be due to experimental errors from the use of single point measurements to determine the phase boundaries as well as a contribution from the diastereomer **2** that is present in the isolated solids. The high stereoisomeric purity across the series of experiments was unexpected because according to the phase diagram; the composition of the systems is in the purple domain in Figure 3 at the end of the process and both **1** and **2** should crystallize. Moreover, a more concentrated solution should also result in a higher yield.

Further resolution tests using strongly stretched conditions (i.e., as low as 5 mL/g of solvent, seeding with **1**, cooled to −2.5 °C, and held for 60 min—entry 5 in Table 5) resulted in the production of **1** crystals with diastereomer **2** content of only 1.3% and with a yield of 41%. However, using 10 mL/g of solvent, cooling down to 2.5 °C and seeding with diastereomer **2** resulted in a product yield of 60% containing 30.8% of **2** (entry 6 in Table 5).

We suggest that the unexpectedly high stereoisomeric purities of the isolated **1** crystals is due to strong predominance of **1** seed growth during cooling (i.e., entrainment effect) over nucleation and growth events of **2**, since seeding the slurry with the undesired enantiomer **2** did not result in significant decrease of the optical purity of **1** crops. Moreover, the absence of yield improvement between entries 1 to 4 in Table 4 (i.e., upon increasing concentration) actually suggests that both diastereomers are significantly reducing the growth of each other. So far this behavior has not been further explained and would require a comprehensive study of the solution crystallization behavior of both **1** and **2**, and in particular their mixtures, to provide complete process understanding. Nevertheless, these first crystallization trials prompted us to perform the resolution procedure under kinetic rather than thermodynamic control in order to further improve the productivity of the process. The robustness of the process using less solvent than required by point **F** was therefore investigated.

Robustness Studies. A 2^{4-1}_{IV} experimental design (DoE) was run that allowed us to investigate the effect of varying the different factors shown in Table 6 in order to assess the robustness of the process at the manufacturing scale. To account for any synthesis yield variations, the stoichiometry of L-(−)-malic acid was also considered since the manufacturing protocol consists of adding the resolving agent to the racemic free base **27**, previously isolated as a solution in ethyl acetate. An additional "stressing" experiment was also included (Table 7, entry 12) where all factors most likely to crystallize

DOI: 10.1021/acs.oprd.5b00283
Org. Process Res. Dev. XXXX, XXX, XXX−XXX

Table 6. Robustness Experimental Design

	factors			
	A	B	C	D
setting	solvent (mL/g)	L-(−)-malic acid (equiv)	cooling rate (°C/min)	final temperature (°C)
low	8	0.9	0.2	15
mid	10	1.0	0.35	20
high	12	1.1	0.5	25

Table 7. Summary of Results

	factors				responses	
	A	B	C	D		
entry no.	solvent (mL/g)	cooling rate (°C/min)	final temp (°C)	L-(−)-malic acid (equiv)	yield (% th)	diastereomer **2** (% a/a GC)
1	8	0.2	15	0.9	39.1	1.14
2	12	0.2	15	1.1	38.8	0.82
3	8	0.5	15	1.1	38.8	1.06
4	12	0.5	15	0.9	39.5	1.38
5	8	0.2	25	1.1	35.1	0.72
6	12	0.2	25	0.9	36.2	0.92
7	8	0.5	25	0.9	36.2	1.21
8	12	0.5	25	1.1	36.9	1.04
9	10	0.35	20	1	38.0	1.03
10	10	0.35	20	1	37.9	0.99
11	10	0.35	20	1	38.1	1.05
12[a]	8	0.5	15	1.1	39.1	1.23

[a]Stressed experiment not included in statistical analysis.

diastereomer **2** were set at the extreme of the investigated range. The experiment was seeded with **2** at 15 °C after the initial crystallization and was held for 18 h to test if elevated levels of **2** would be detected.

Results from the experiments run, including three center-points, are shown (Table 7). Using the software Design-Expert (version 7.1.1, Stat-Ease, Inc.) models for yield and diastereomer content were obtained. For yield, a significant model was obtained (R^2 = 0.8965, adj R^2 = 0.8835, pred R^2 = 0.8155). A half-normal plot showed that temperature was the only significant factor (Figure 9) with lower temperature giving an increased yield. For diastereomer content, a significant model was also obtained (R^2 = 0.9869, adj R^2 = 0.9765, pred R^2 = 0.9353). A half-normal plot (Figure 9) showed that cooling rate and L-(−)-malic acid were the most significant effects with slower cooling rate and higher L-(−)-malic acid giving lower diastereomer content. Final temperature shows a small effect with a higher temperature resulting in lower diastereomer content and there is a small temperature and L-(−)-malic acid interaction. Varying solvent quantity within the range studied had no significant effect. Reassuringly, no significantly elevated levels of **2** were seen in the stress experiment.

The results established that it was not possible to completely remove all undesired diastereomer **2** in a single resolution step by means of any of the process parameters, which first raised suspicions of the presence of a narrow domain of solid solution isomorphism to **1**.

Recrystallization Studies. Given that the stringent target specification of chiral purity (<0.15% of counter-enantiomer) could not be achieved directly from the resolution, a recrystallization process was developed based on the minimum quantity of ethyl acetate to dissolve the product at reflux. The process consisted of dissolving the impure material in 10 mL/g of ethyl acetate at reflux, followed by a cooling step from 70 to 15 °C at 0.5 °C/min, aging, and filtration. The wet cake was washed with ethyl acetate and dried under reduced pressure. This process was shown to efficiently purge **2** from **1** samples, which (considering that this crystallization is not seeded with **1**) rules out the existence of any stable domains of solid solutions in the binary system of **1** and **2**. The elevated content of **2** after the first resolution step is therefore likely due to kinetic effects during crystallization.

To confirm the robustness of this recrystallization process, a further DoE was run, varying the factors shown in Table 8 with

Table 8. Recrystallization Experimental Design

setting	solvent (mL/g)	cooling rate (°C/min)	final temperature (°C)	diastereomer **2** (% a/a GC)
low	8	0.2	5	1.3
mid	10	0.35	15	2.0
high	12	0.5	25	2.7

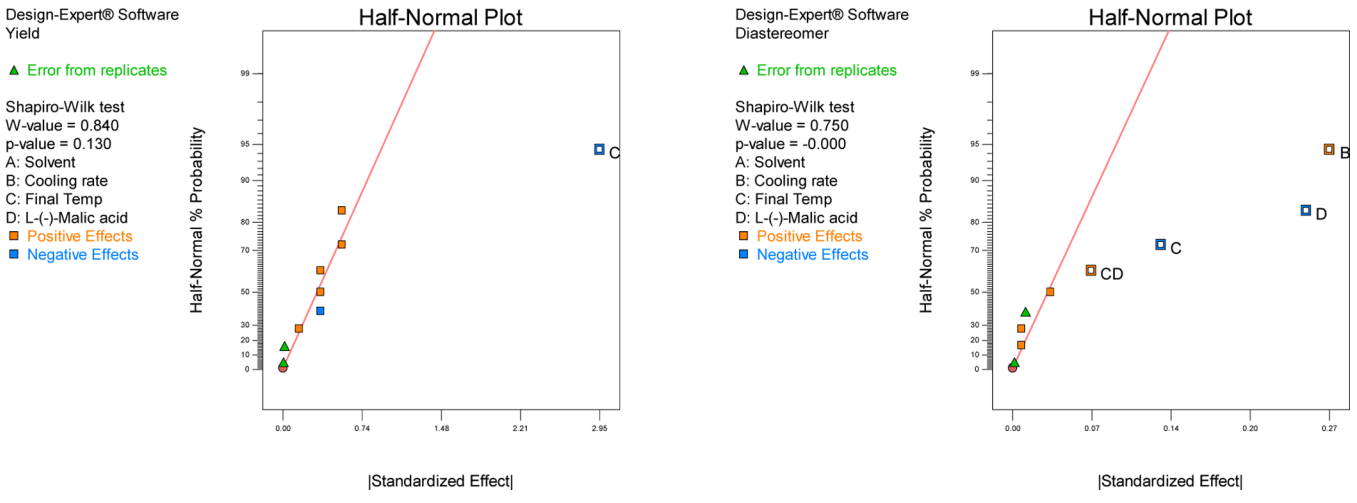

Figure 9. Half-normal plots for yield (left) and diastereomer content (right).

DOI: 10.1021/acs.oprd.5b00283
Org. Process Res. Dev. XXXX, XXX, XXX−XXX

those factors kept constant shown in Table 9. The diastereomer content of the input material was varied within a range

Table 9. Constant Factors for Recrystallization Design

factor	value
solution temperature	reflux (ca. 77 °C)
hold temperature	70 °C
hold time at 70 °C	15 min
final age time	60 min
filter cake wash	2 × 2 mL/g

somewhat higher than we routinely expected to achieve on scale. The results obtained are shown in Table 10.

The results of our DoE were very consistent across the range of experiments with respect to recoveries (i.e., variations between 94.1% and 96.8%) and diastereomer content (i.e., below 0.1% in every case). The chiral purity of the input material was the only significant source of variation evidenced by the DoE, but since this parameter was expected to be controlled well below 2% via the first resolution, the recrystallization was expected to provide an excellent level of stereochemical purity at the manufacturing scale.

Manufacturing Scale Results. The reductive amination followed by the resolution and subsequent recrystallization was scaled up in the GSK Jurong Pilot Plant (Singapore) starting with 50 kg of acetophenone derivative **11** per batch (Scheme 7). The typical conversion of **11** to racemate **27** in solution had previously been determined to be 96% after quench and workup. As a result a standard charge of 0.96 equiv of L-(−)-malic acid (based on input **11**) was added as resolving agent to the process, equal to 1.00 equiv of L-(−)-malic acid vs expected solution yield of **27**. Campaign results are shown in Table 11.

CONCLUSIONS

We have developed an optimized process to obtain a key building block required for the manufacture of vestipitant that is suitable for ongoing large-scale manufacture. The early stages of chemistry have been substantially simplified, and design of experiments and time coursing studies have been used to develop a good understanding of the behavior of the system. The Pasteurian resolution of the racemic mixture has been established through the use of ternary phase diagrams that were simply constructed from a series of single solubility experiments and allowed the rapid screening and evaluation of the resolution conditions to deliver a robust and efficient crystallization with minimal effort. Overall the sequence offers significant advantages in terms of operational simplicity, robustness, and freedom to operate and has been successfully demonstrated on the intended commercial scale, delivering the desired product with exquisite stereochemical purity.

EXPERIMENTAL SECTION

General Methods. NMR: spectra (^{1}H) were recorded on a Bruker Avance spectrometer at 400 MHz. GC method: Column, Agilent DB5-HT; oven temperature program, 50 °C (hold for 5 min), ramp 1 75 °C/min to 320 °C (hold for 2.5 min), ramp 2 −300 °C/min to 50 °C; air flow 450 mL/min, hydrogen flow 40 mL/min, makeup flow 25 mL/min; flow mode, constant pressure, initial pressure 30 psi; injector temperature 275 °C; injection volume 1.0 μL (split ratio 100:1); detection FID; detector temp 320 °C; detector constant makeup flow. Sample preparation, 0.5−5 mg/mL analyte in acetonitrile. Chiral GC method: column, Chirasil-dex CB 25 m × 0.25 mm capillary, 0.25 μm film thickness; carrier gas, helium; gas flow, 1 mL/min; injector temperature, 250 °C; oven temperature program, 80 °C (hold for 6 min), ramp 10 °C/min to 160 °C, column equilibration time, 3 min; injection volume, 1 μL (split ratio 20:1); FID detector temperature, 275 °C; makeup gas, nitrogen; makeup flow 25 mL/min; fuel (hydrogen) flow, 40 mL/min; air flow, 400 mL/min; run time 14 min. Sample preparation: add approx 10 mg of salt to 1 mL of toluene and 2 mL of 2 M sodium hydroxide solution and sample upper toluene layer. Retention times: **1**, approx 9.6 min; **2**, approx 9.4 min. HPLC method: column, Agilent Zorbax SB C18, 1.8 μm, 50 × 3.0 mm; mobile phase A was 0.05% (v/v) trifluoroacetic acid in water, and mobile phase B was 0.05% (v/v) trifluoroacetic acid in acetonitrile; gradient method (100% A to 95% B over 2.5 min) was used at 1.5 mL/min; detection 210 nm. Software: Experimental designs were planned and evaluated using Design-Expert 7.1.1 (Stat-Ease, Inc. Minneapolis).

(R)-3,5-Bis(trifluoromethyl)-α-methyl-N-methylbenzylamine L-(−)-Malic Acid Salt (1). To a nitrogen inerted solution of 3′,5′-bis(trifluoromethyl)acetophenone (**11**) (50 kg, 195.2 mol) in methanol (300 L) was charged an aqueous solution of 40% (w/w) methylamine (50 kg, 3.3 equiv). The stirred solution was heated to 35 °C for 6 h. The solution was cooled to 0 °C over 2 h and was stirred for 10 h. GC confirmed that <5% **11** remained. Sodium borohydride (total of 9 kg, 1.2 eq) was added in portions with cooling to maintain at 0 ± 5 °C.

Table 10. Recrystallization DoE Results

	factors				responses	
entry	solvent (mL/g)	cooling rate (°C/min)	final temperature (°C)	input diastereomer **2** (%)	yield (% th)	diastereomer **2** (% a/a GC)
1	8	0.2	5	1.3	96.1	0.03
2	12	0.2	5	2.7	96.8	0.07
3	8	0.5	5	2.7	96.8	0.09
4	12	0.5	5	1.3	95.8	0.04
5	8	0.2	25	2.7	95.0	0.06
6	12	0.2	25	1.3	94.7	0.03
7	8	0.5	25	1.3	95.3	0.03
8	12	0.5	25	2.7	94.1	0.07
9	10	0.35	15	2.0	95.9	0.05
10	10	0.35	15	2.0	96.5	0.04
11	10	0.35	15	2.0	95.5	0.05

DOI: 10.1021/acs.oprd.5b00283
Org. Process Res. Dev. XXXX, XXX, XXX−XXX

Scheme 7. Final Manufacturing Process of 1.

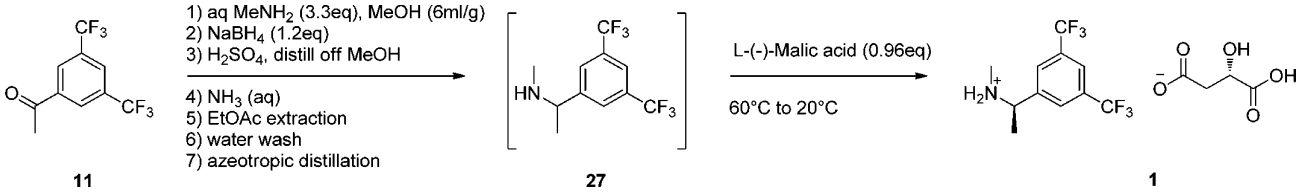

Table 11. Manufacturing Campaign Results

	racemate synthesis and resolution			recrystallization		
batch	yield (kg)	yield (% th)	diastereomer **2** (% a/a GC)	yield (kg)	yield (% th)	diastereomer **2** (% a/a GC)
1	26.8	33.9	0.79	22.9	85.4[a]	not detected
2	26.7	33.7	0.85	24.6	92.3	<0.05[b]
3	27.4	34.7	0.94	26.0	94.9	<0.05[b]
4	27.1	34.2	0.83	25.2	93.0	<0.05[b]

[a]Reduced yield due to losses to filter dryer "heel". [b]Above limit of detection but measured at <0.01%. The formal validated limit of quantification is 0.05%.

(Add 6 × 0.5 kg at 15 min intervals and 2 × 3 kg at 30 min intervals.) Each 3 kg portion was rinsed in with methanol (3 L). The mixture was heated to 25 °C and was stirred for 30 min. HPLC confirmed the reaction as complete. 5 M sulfuric acid (101 L) was added over 2 h with cooling to control temperature up to 40 °C and the rate of hydrogen evolution. Final pH ∼ 3. The solution was heated to reflux (ca. 71 °C), and after 15 min hydrogen evolution ceased. The solution was cooled to 40 °C and was diluted with water (60 kg). Solvent was removed by distillation at atmospheric pressure to a total volume of 300 L. Water (140 L) was added, and the solution was again distilled to 300 L total volume. The solution was cooled to 40 °C, and 26% w/w ammonia solution (90 L) was added with cooling to maintain temperature. The solution was extracted with ethyl acetate (200 L), and the organic extract was distilled to a total volume of 150 L. The solution was azeotroped dry with further distillations of ethyl acetate (3 × 25 L) to water content <0.2% (w/w) (Karl Fisher). Ethyl acetate (400 L) and L-(−)-malic acid (25 kg, 0.96 equiv) were added, and the mixture was heated to 60 °C to give a clear solution. The solution was cooled to 50 °C, and a seed of pure **1** (0.25 kg) as a slurry in ethyl acetate (1 L) was added. The mixture was stirred for 1 h, cooled to 20 °C over 90 min, and then stirred for 1 h. The resulting slurry was filtered and was washed with fresh ethyl acetate (3 × 100 L). The product was dried under reduced pressure at 50 °C to yield **1** as a white crystalline solid (27.05 kg, 34.2% th yield). Chiral GC shows 0.79−0.94% enantiomer.

Recrystallization. Crude **1** (27.05 kg) was dissolved in ethyl acetate (271 L) at reflux. The clear solution was cooled to 67 °C and was stirred for 30 min to initiate crystallization. The suspension was cooled to 15 °C over 150 min and was stirred for 60 min. The resulting slurry was filtered, washed with ethyl acetate (108 L), and dried under reduced pressure at 50 °C to yield pure **1** (25.15 kg, 93% th yield). ^{1}H NMR (400 MHz, d_6-DMSO) δ 1.45 (d, J = 6.6 Hz, 3H), 2.34 (s, 3H), 2.34−2.39 (m, 1H), 2,56 (dd, J = 7.8 Hz, 1H), 4.05 (dd, J = 7.8, 5.6, 1H), 4.26 (q, J = 6.6, 1H), 8.08 (s, 1H), 8.17 (s, 2H). Chiral GC shows < 0.05% enantiomer.

AUTHOR INFORMATION

Corresponding Author

*E-mail: david.r.stevens@gsk.com

Notes

The authors declare no competing financial interest.

ACKNOWLEDGMENTS

We thank Prof. Gérard Coquerel for useful discussions of our results. We would like to thank the entire project team, in particular Caroline Tudge and Martin Collier-Smith (Analysis), Lesley Senior (PAT), and Andrew Payne (Process Safety) for their support of this work.

REFERENCES

(1) (a) Di Fabio, R.; Griffante, C.; Alvaro, G.; Pentassuglia, G.; Pizzi, D. A.; Donati, D.; Rossi, T.; Guercio, G.; Mattioli, M.; Cimarosti, Z.; Marchioro, C.; Provera, S.; Zonzini, L.; Montanari, D.; Melotto, S.; Gerrard, P. A.; Trist, D. G.; Ratti, E.; Corsi, M. *J. Med. Chem.* **2009**, *52*, 3238−3247. (b) Guercio, G.; Bacchi, S.; Perboni, A.; Leroi, C.; Tinazzi, F.; Bientinesi, I.; Hourdin, M.; Goodyear, M.; Curti, S.; Provera, S.; Cimarosti, Z. *Org. Process Res. Dev.* **2009**, *13*, 1100−1110.

(2) (a) Di Fabio, R.; Alvaro, G.; Griffante, C.; Pizzi, D. A.; Donati, D.; Mattioli, M.; Cimarosti, Z.; Guercio, G.; Marchioro, C.; Provera, S.; Zonzini, L.; Montanari, D.; Melotto, S.; Gerrard, P. A.; Trist, D. G.; Ratti, E.; Corsi, M. *J. Med. Chem.* **2011**, *54*, 1071−1079. (b) Cimarosti, Z.; Bravo, F.; Castoldi, D.; Tinazzi, F.; Provera, S.; Perboni, A.; Papini, D.; Westerduin, P. *Org. Process Res. Dev.* **2010**, *14*, 805−814.

(3) Christensen, S. R.; Merlo Pich, E.; Ratti, E.; Yamada, T. Preparation of Carbamoylpiperazine Derivatives as NK1 Receptor Antagonists, International Patent Application WO 2008/046882, April 24, 2008; *Chem. Abstr.* 2008, *148*, 495980.

(4) ICHQ11 http://www.ich.org/products/guidelines/quality/article/quality-guidelines.html (accessed Oct 30, 2015).

(5) Hodges, G. R.; Martin, J; Hammil, N. A.; Houson, I. N. Process for Preparation of N-(arylmethyl)amine by Stereoselective Reduction of Aryl Ketone to Chiral Arylmethanol Derivative. International Patent Application WO 2006/067395, June 29, 2006; *Chem. Abstr.* 2006, *145*, 103419.

(6) Xie, J.-H.; Liu, X.-Y.; Xie, J.-B.; Wang, L.-X.; Zhou, Q.-L. *Angew. Chem., Int. Ed.* **2011**, *50*, 7329−7332.

(7) Tanaka, T.; Okuro, K.; Mitsuda, M. Method for Producing Optically Active Benzylamine Derivative. International Patent Application WO 2007/037242, April 5, 2007; *Chem. Abstr.* 2007, *146*, 379671.

(8) Ishii, A.; Motegi, K.; Tsuruta, H.; Inomiya, K. Method for producing optically active N-alkyl-N-[1-(fluoro, trifluoromethyl or trifluoromethoxyphenyl)alkyl]amine. International Patent Application WO 2008/001719, Jan 3, 2008; *Chem. Abstr.* 2008, *148*, 121451.

(9) Jones, S.; Li, X. Preparation of 1-(azolylcarbonyl)-2-(methoxymethyl)pyrrolidines for use as catalysts for asymmetric reduction of imines. International Patent Application WO 2013/079942, June 6, 2013; *Chem. Abstr.* 2013, *159*, 75891.

(10) DSM (No inventor data available), Process for the production of chiral amines using iridium-catalyzed asymmetric hydrogenation as key step. European Patent Application EP 2363388, September 7, 2011; *Chem. Abstr.* 2011, *155*, 406856.

DOI: 10.1021/acs.oprd.5b00283
Org. Process Res. Dev. XXXX, XXX, XXX−XXX

(11) Imamoto, T.; Tamura, K.; Zhang, Z; Horiuchi, Y.; Sugiya, M.; Yoshida, K.; Yanagisawa, A.; Gridnev, I. D. *J. Am. Chem. Soc.* **2012**, *134*, 1754−1769.
(12) Levilain, G.; Coquerel, G. *CrystEngComm* **2010**, *12*, 1983−1992.
(13) Viedma, C.; McBride, J. M.; Kahr, B.; Cintas, P. *Angew. Chem.* **2013**, *125*, 10739−10742.
(14) Tamura, R.; Fujimoto, D.; Lepp, Z.; Misaki, K.; Miura, H.; Takahashi, H.; Ushio, T.; Nakai, T.; Hirotsu, K. *J. Am. Chem. Soc.* **2002**, *124*, 13139−13153.
(15) Pasteur, L. *C. R. Acad. Sci.* **1853**, *37*, 162−166.
(16) Coquerel, G. Preferential Crystallization. In *Novel Optical Resolution Technologies*; Sakai, K., Hirayama, N., Tamura, R., Eds.; Top. Curr. Chem.; Springer-Verlag: Berlin, 2007; Vol. *269*, pp 1−51.
(17) Ricci, J. E. *The Phase Rule and Heterogeneous Equilibrium*; D. Van Nostrand Company: New York, 1951.
(18) (a) Jacques, J.; Collet, A.; Wilen, S. H. *Enantiomers, Racemates and Resolutions*; Krieger Publishing Company: Malabar, FL, 1994. (b) Querniard, F.; Linol, J.; Cartigny, Y.; Coquerel, G. *J. Therm. Anal. Calorim.* **2007**, *90*, 359−365. (c) Brandel, C.; Amharar, Y.; Rollinger, J. M.; Griesser, U. J.; Cartigny, Y.; Petit, S.; Coquerel, G. *Mol. Pharmaceutics* **2013**, *10*, 3850−3861.
(19) At the thermodynamic equilibrium, a slurry of a defined compound <AB> presenting a congruent solubility gives rise to a mother liquor with an equimolar ratio of A and B, and the nature of the solid phase in suspension is unchanged. By contrast, a slurry of a defined compound <AB> presenting a noncongruent solubility gives rise to a mother liquor with a different molar ratio of A and B and the solid phase in suspension is no longer pure <AB>.
(20) Marchand, P.; Lefèbvre, L.; Querniard, F.; Cardinaël, P.; Perez, G.; Counioux, J.-J.; Coquerel, G. *Tetrahedron: Asymmetry* **2004**, *15*, 2455−2465.
(21) The imine is not stable under HPLC conditions, but ^{1}H NMR and GC were found to be suitable.
(22) In common with most borohydride reductions, the exact behaviors of the hydride species in solution are not well understood at this time.
(23) Barrett, R.; Caine, D. M.; Cardwell, K. S.; Cooke, J. W. B.; Lawrence, R. H.; Scott, P.; Sjolin, Å. *Tetrahedron: Asymmetry* **2003**, *14*, 3627−3631.

DOI: 10.1021/acs.oprd.5b00283
Org. Process Res. Dev. XXXX, XXX, XXX−XXX